Two-axis optical fiber acclerometer

C. DOYLE, G. F. FERNANDO
Engineering Systems Department, Cranfield University (RMCS), Shrivenham, Swindon, SN6 8LA, UK

The authors have previously demonstrated the design and evaluation of an optical fiber-based vibration sensor for impact damage detection in fiber reinforced composites [1]. This current paper demonstrates a further development of the original vibration sensor into a small, intensity-modulated, 2-axis, passive accelerometer. Fiber-optic vibration sensors offer the possibility of monitoring the in-service performance and structural integrity of engineering materials and machinery in hostile and hazardous environments. Much recent work has been done on optical fiber sensors which may be employed in areas with high voltages, strong electromagnetic fields, explosive or flammable atmospheres, any of which may preclude the use of current piezoelectric or capacitative devices.

For applications requiring vibration or acceleration monitoring in two or more directions, the traditional approach is to mount single-axis devices, which may be of any type, perpendicularly. Examples of multi-axis fiber-optic sensors include that of Schröpfer *et al.* [2], who combined three micromachined seismic masses on a single silicon chip, with interferometric interrogation. Dinev [3] employed a single cylindrical cantilever as an inertial mass giving two axes of sensitivity, but his device was relatively large (≈160 mm long) and was not entirely passive, as it contained a position sensitive photodetector. A smaller sensor could be made by employing a cantilevered bare fiber as the sensitive element. Morante *et al.* [4] performed a comprehensive theoretical treatment of a bare optical fiber as an accelerometer and based on their analysis they made a single-axis accelerometer in which light exiting the cantilevered fiber fell on two receiving fibers. A perfectly symmetrical optical fiber would have equal response to all accelerations in the plane perpendicular to its axis, permitting it to form the sensing element in a 2-axis device.

As shown in Fig. 1, a cantilevered optical fiber is employed as the inertial mass and light exiting its free end falls on four receiving fibers. The position of the end of the cantilevered fiber, and hence the direction and magnitude of the applied acceleration, is obtained from the relative optical power coupled into each of the receiving fibers. Good alignment of the fibers is ensured by using precision-drawn silica tubes to support the sensing fiber and hold the receiving fibers in position. Step index 100/125 multimode fibers with a numerical aperture (NA) of 0.22 maximize light throughput and give greater tolerance to small misalignments. The sensor is assembled in a fusion splicer equipped with a 2-axis viewing microscope and stepper motor translation stages and is fixed together with UV-cured epoxy resin.

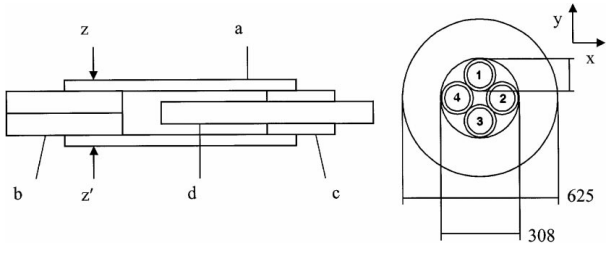

Figure 1 Schematic diagram of the sensor (left) and section z-z′, showing numbering of fibers (right). Key: a) outer housing; b) receiving fibers; c) support tube and d) cantilevered input fiber. Dimensions in microns.

Due to different splice or connector losses, or variations in detector sensitivity, the four optical signals may differ in intensity. Therefore a referencing step is first performed, in which each input signal is normalized by dividing by the signal level in the absence of any acceleration, giving four signals each having a mean value of one. One way to find the offset between the end of the cantilevered fiber and each of the receiving fibers requires determination of the appropriate coupling curve (i.e. the relationship between transverse displacement and power coupled into the receiving fiber, with the two fibers at a constant axial separation). Lopez-Higuera *et al.* [5] fitted a straight line to this curve, giving an error of ±0.5% over a range of ±5 μm. The alternative demodulation method described below may be employed to obtain acceleration over a greater range of displacements of the cantilevered fiber.

With x- and y-directions as defined in Fig. 1 we can see that increasing x-displacement will be some function of $(P_2 - P_4)$, and increasing y-displacement will be a function of $(P_1 - P_3)$, where P_i is the normalized optical power coupled into the ith receiving fiber. However, for a given y-position the intensities $P_{1,3}$ will decrease with increasing displacement in x. There will be a corresponding change in $P_{2,4}$ with displacement in y. To compensate for this, we increase each of the basic intensity differences, $(P_1 - P_3)$ and $(P_2 - P_4)$, by some multiple of the magnitude of the function in the perpendicular direction. This gives two similar equations:

$$\begin{aligned} y &= C\{(P_1 - P_3) + k(P_1 - P_3)|P_2 - P_4|\} \\ x &= C\{(P_2 - P_4) + k(P_2 - P_4)|P_1 - P_3|\} \end{aligned} \quad (1)$$

where in the y-direction, for example, the multiplying constant k corrects for the reduction in both P_1 and P_3 for positive or negative x-displacements. For a symmetrical sensor, the same value of k applies in the x-direction, and C is a calibration factor which translates the intensity equations above into movement

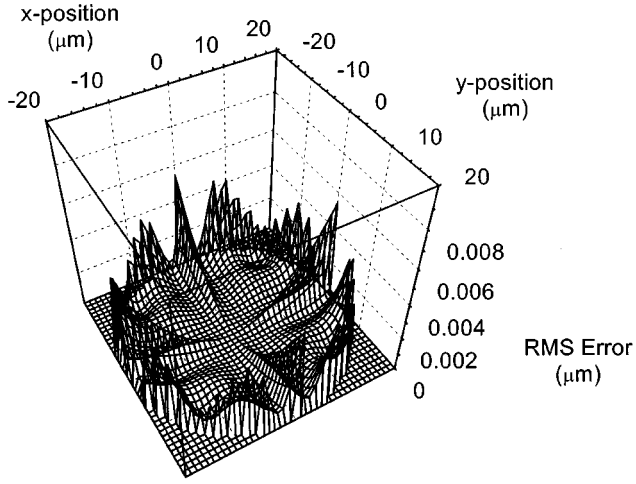

Figure 2 RMS error of simple demodulation scheme compared with values obtained from consideration of the measured power coupling curve (100 mm step-index fibers at 600 mm axial separation).

of the fiber end or directly into acceleration. The extent of nonlinearity of the coupling curve sets the displacement range over which this approximate method may be employed for a given tolerable error. In particular, this method works well if the region of interest of the coupling curve contains no general points of inflexion.

This demodulation scheme was tested theoretically by producing a set of expected optical signals, using previously measured results of power coupled between fibers. This test set was compared with the answers obtained by the simple demodulation scheme outlined above and the difference between the two plotted against position in Fig. 2. The constants k and C were calculated iteratively in order to minimize the RMS error over a range of 20 μm in all directions. The overall RMS error was 0.00123 μm, reducing further for smaller displacements.

A sensor was made with a cantilevered fiber 12.4 mm long, giving a resonant frequency of 592 Hz and theoretical sensitivity to acceleration, in terms of motion of the free end with applied acceleration, of 1.1 μm g^{-1}. It was cemented into a grooved cylinder, which was then clamped onto the table of an electromagnetic shaker (LDS V-201), along with a reference piezoelectric accelerometer (Endevco model 224c). The input fiber was

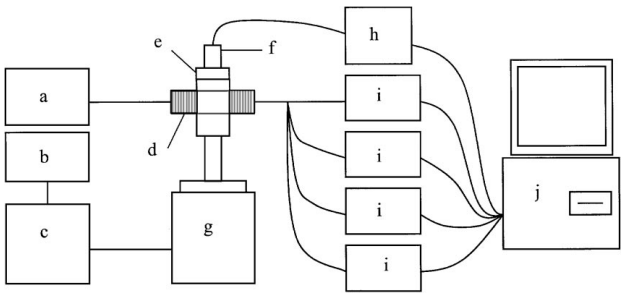

Figure 3 Arrangement for testing 2-axis sensor. Key: a) white light source; b) signal generator; c) power amplifier; d) sensor; e) test fixture allowing rotation of (d); f) reference accelerometer; g) electromagnetic shaker; h) charge amplifier; i) photodiodes and amplifiers; and j) PC for data acquisition.

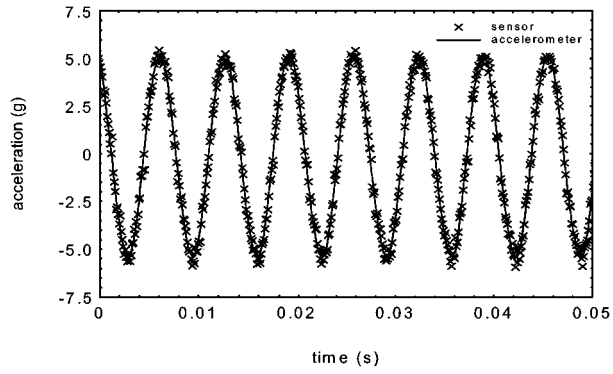

Figure 4 Example of sensor and reference accelerometer outputs at 150 Hz.

illuminated with a 10 W tungsten halogen source with an NA of 0.4. A sinusoidal drive signal was applied to the shaker and the four optical and one accelerometer outputs were sampled at 10 kHz each with a PC-based data acquisition system. The experimental layout is illustrated in Fig. 3. The value of C was chosen to minimize the error between the sensor and the reference accelerometer and k was as determined above. For the tested sensor, $C = 17.2711$ and $k = 0.0277$. Fig. 4 presents examples of sensor and accelerometer outputs. Notice that the mean level of both signals is displaced downward from zero by 1 g, due to gravity. The sensor was excited at 100 Hz and from ± 0.75 to ± 8 g peak-to-peak (p-p). The sensor output is plotted against that of the accelerometer in Fig. 5. The linearity is good with a linear regression fit through the origin giving a slope of 0.998. The scatter may be attributable to the relatively low power light source used, giving a poor signal-to-noise ratio. The cylinder mounting the sensor was rotated a full circle in 30° steps about its axis and tested at 100 Hz, ± 5 $g_{p\text{-}p}$. Fig. 6 is a plot of the direction of excitation indicated by the sensor against the actual angle. The x-error bars span $\pm 3°$, reflecting the estimated imprecision in setting the angle of the sensor. The RMS error between the sensor output and the desired angle is 2.92° and a linear regression fit through the data has a slope of 1.00 and passes through the origin.

The proposed sensor displays good amplitude linearity and directional resolution. Only cheap instrumentation and simple signal processing are required.

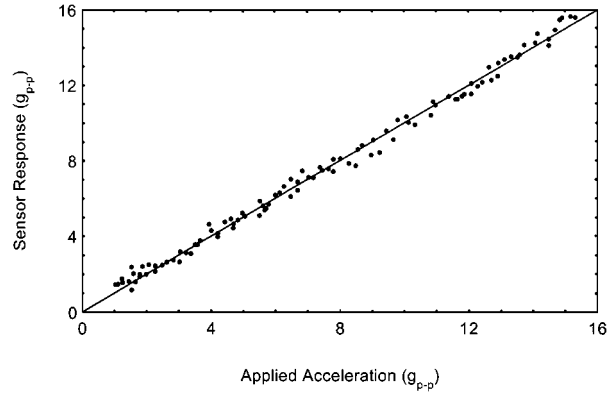

Figure 5 Sensor output vs. magnitude of applied acceleration as given by the reference accelerometer. At 100 Hz, 0 degrees.

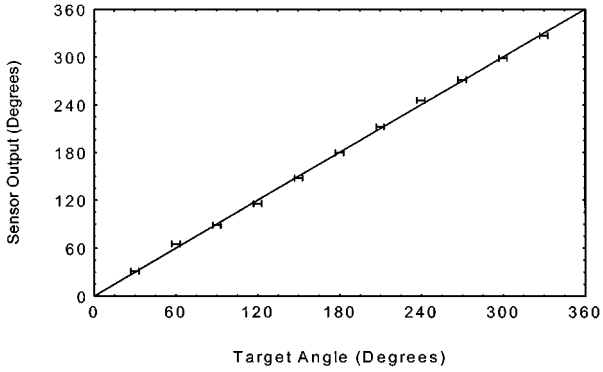

Figure 6 Sensor output vs. angle of applied acceleration at 100 Hz, 10 $g_{p\text{-}p}$.

The sensor head is entirely passive and hence intrinsically safe. This system has considerable scope for optimization. The range and natural frequency of the sensor can be controlled by choosing the length and diameter of the cantilevered fiber. The shape of the coupling curve, hence the sensitivity of the demodulation system, is a function of the power distribution exiting the sensing fiber and the NA and geometry of the receiving fibers. The former is determined by the source, launch conditions, length and fiber NA. Wavelength-division multiplexing could combine the four return signals down a single fiber, facilitating common-mode rejection of errors induced by perturbation of the signal fiber and this suggests the possibility of operating several sensors with one fiber. Packaging issues would have to be addressed in any practical device.

Acknowledgments

This work was funded by the EPSRC and Mr. W. Ridoutt of Cape Durasteel. The authors thank Professor B. Ralph and Dr. P. Crosby for their assistance.

References

1. C. DOYLE and G. FERNANDO, *J. Mater. Sci. Lett.* **16** (1997) 1104.
2. G. SCHRÖPFER, W. ELFLEIN, M. DE LABACHELERIE, H. PORTE and S. BALLANDRAS, *Sensors and Actuators A* **68** (1998) 344.
3. P. D. DINEV, *Rev. Sci. Instrum.* **67**(1) (1996) 288.
4. M. MORANTE, A. COBO, J. M. LOPEZ-HIGUERA and M. LOPEZ-AMO, *Opt. Eng.* **35**(4) (1996) 1700.
5. J. M. LOPEZ-HIGUERA, M. MORANTE and A. COBO, *J. Lightwave Tech.* **15**(7) (1997) 1120.

Received 27 August
and accepted 10 December 1999